1. Hamza FEROURA[1], 2. Fateh KRIM[1], 3. Abdelouahad MAY[1], 4. Abdesslam BELAOUT[2]

Department of Electronics, Laboratory of Power Electronics and Industrial Control (LEPCI), University of Setif-1, Setif, 19000, Algeria. (1)
Research Center in Industrial Technologies CRTI, P.O. Box 64, Cheraga, Algiers, 16014, Algeria. (2)
ORCID: 1. 0000-0002-0946-1060; 2. 0000-0001-9529-5291; 3. 0000-0002-8922-7409; 4. 0000-0002-9536-6149

Model Predictive Control Based PV Grid-Connected Single-stage Three Phase Split-Source Inverter

Abstract. Single-stage power conversion systems with boosting capabilities offer some important advantages. Among various alternatives, the split-source inverter (SSI) has recently garnered attention as a potential alternative to the commonly employed Z-source inverter. This paper proposes a model predictive control (MPC) algorithm for grid integration of photovoltaic (PV) systems using a three phase SSI. SSI is similar to conventional voltage source inverter (VSI) and requires the same number of power switches with three additional diodes connected between the input source through an inductor and the nodes of each inverter leg. The proposed finite control-set model predictive controller (FCS-MPC) uses a discrete-time model of the system in order to predict its future behaviour for each of the finite states, then the optimal control action is chosen by minimizing a suitable cost function. Simulation results presented in this paper demonstrate the feasibility and the good performance of the proposed system.

*Streszczenie. Jednostopniowe systemy konwersji mocy z możliwością zwiększania mocy oferują kilka ważnych zalet. Wśród różnych alternatyw, ostatnio uwagę zwraca falownik z dzielonym źródłem (SSI) jako potencjalna alternatywa dla powszechnie stosowanego falownika ze źródłem Z. W artykule zaproponowano model algorytmu sterowania predykcyjnego (MPC) do integracji sieci systemów fotowoltaicznych (PV) z wykorzystaniem trójfazowego SSI. SSI jest podobny do konwencjonalnego falownika źródła napięcia (VSI) i wymaga takiej samej liczby przełączników mocy z trzema dodatkowymi diodami podłączonymi pomiędzy źródłem wejściowym poprzez cewkę indukcyjną a węzłami każdej nogi falownika. Proponowany sterownik predykcyjny modelu skończonego zbioru sterowania (FCS-MPC) wykorzystuje dyskretny model systemu w celu przewidzenia jego przyszłego zachowania dla każdego ze skończonych stanów, następnie wybierane jest optymalne działanie sterujące poprzez minimalizację odpowiedniej funkcji kosztu . Wyniki symulacji przedstawione w tym artykule wykazują wykonalność i dobrą wydajność proponowanego systemu. (**Model Predykcyjnej Kontroli Opartej na Sieci PV Jednofazowy Trójfazowy Falownik Split-Source Podłączony do Sieci**)*

Keywords: Photovoltaic (PV); Single-stage; Split-source inverter (SSI); Model predictive control (MPC).
Słowa kluczowe: Fotowoltaika (PV); Pojedyncza scena; Falownik z dzielonym źródłem (SSI); Modelowa kontrola predykcyjna (MPC).

Introduction

The Electric energy consumption has been growing significantly during the past few years to address the energy needs associated with the expanding global population and rapid economic expansion. Currently, the majority of electricity is produced by burning fossil fuels leading to global climate change. Over the past few decades, there has been a steady rise in demand for clean, economic and renewable energy, particularly as a result of the energy crisis and environmental issues such as pollution and global warming [1, 2].

Due to its availability and clean conversion to electricity via the photovoltaic process, solar energy appears to be a leading contender among various renewable energy sources available [3].

Regarding power electronic converters to interface PV arrays to the grid, voltage source inverter (VSI) is the most used topology to date. However, this topology has some limitations when it comes to PV applications. In such PV applications, the required AC voltage exceed the DC input voltage. Since the VSI topology has buck (step-down) characteristics, an extra DC-DC boost converter is required, this configuration is known as dual-stage. On the other hand, single stage architectures are recently gaining importance due to their merits in terms of cost, size, and complexity of the whole system.

Many inverter topologies have been designed to fulfil the requirement of these architectures. The most common topologies are current source inverter (CSI), impedance source inverter (ZSI), quasi-impedance source inverter (qZSI) [1]. Alternatively, a new topology referred to as Split-source inverter (SSI) was recently proposed [4], this topology compared to ZSI have the following advantages: continuous input current, a standard modulation strategy that employs the same eight states of the VSI, and a constant inverter voltage with a low frequency component [4, 5]. The single-stage configuration of SSI requires simultaneously addressing two control objectives, namely, both the DC and AC sides. In literature, SSI is not investigated profusely. After being proposed and analysed in [4], authors in [5] and [6] have introduced controllers based on modified space vector modulation for a grid connected PV system. In the same research direction, authors adopted in [7] a control strategy for a stand-alone SSI system. The research in [8] proposed a peak power controller to deal with the aforementioned control objectives. The paper of [9] examines the common mode voltage (CMV) for a grid connected PV-fed SSI.

MPC was introduced as an advanced control method in the process industry in the 1970s. Formulated in the time domain and suitable for multiple-input multiple-output (MIMO) systems with physical constraints and complex, nonlinear dynamics. However, MPC has not gained attention in the domain of power electronics and converters control before the 2000's. Recently, FCS-MPC is one the most appropriate techniques for the control of converters, due to its good performance, and simplicity of implementation. Typically, FCS-MPC addresses an optimization problem across a finite prediction horizon, selecting the optimal trajectory within that horizon. This search procedure is continued with updated estimations and measurements for the next sampling instant.

Concerning FCS-MPC with SSI in literature, it was only applied to its single-phase version. The paper of [10] presented single phase split source inverter using a model predictive controller based on an energy-function, whereas authors in [11] provided a multi-objective sliding mode combined with MPC.

This work proposes a new PV-fed grid connected three phase SSI using FCS-MPC along with a modified MPPT algorithm. The proposed predictive controller fulfils two control objectives, on one hand, a good quality grid currents with unity power factor operation or with reactive power control depending on grid standards, on the other hand, a

maximum and smooth PV power by controlling the PV current.

This paper is organized as follows: After the introduction, Section 1 introduces the SSI description and modelling, while Section 2 is dedicated to the MPPT algorithm used, whereas in Section 3 the DC-bus voltage regulation is discussed. In Section 4 the decoupled reactive power control method is presented. The proposed FCS-MPC controller is studied in Section 5. Simulation results and discussion are exhibited in Section 6, and finally a conclusion.

SSI Description and Modelling

The SSI is a combination of a boost converter and a voltage source inverter (VSI). It is made up by connecting an input inductor to the switching nodes of VSI phase legs using diodes.

The three phase SSI shown in Fig.1. (a) has the same eight standard operating states as the conventional full bridge VSI. The inductor L is accumulating energy from the input source when one of the lower switches at least is conducting which corresponds to inverter state V_0 to V_6, as illustrated in Fig.1. (b). In contrast, Fig.1. (c) depicts the equivalent circuit when all the upper switches are ON which corresponds to inverter state V_7, the inductor L is discharging and transferring the energy to the capacitor C.

(a)

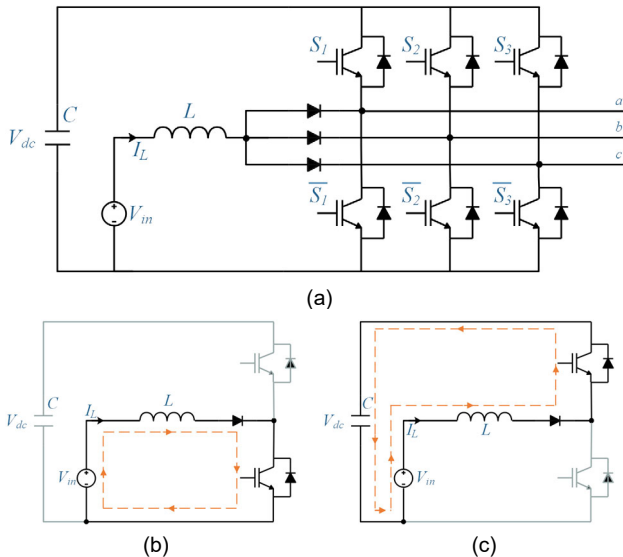(b)   (c)

Fig.1. (a) Three phase SSI, (b) Equivalent circuit during charging of inductor, (c) Equivalent circuit during discharging of inductor.

Hence, the volt-second balance across the input inductor and the DC Bus capacitor is given by

$$(1) \qquad (V_{in} - V_{dc}).t_7 + V_{in}.(T_s - t_7) = 0$$

Where t_7 is the V_7 voltage vector switching time, T_s is the sampling period, V_{in} is the input voltage, and V_{dc} the DC bus voltage.
From (1), the DC Bus voltage can be derived as

$$(2) \qquad V_{dc} = \frac{T_s}{t_7} V_{in}$$

From the last equation, it is obvious that the SSI has the boosting capability, and its DC side acts as a DC-DC boost converter, whose duty cycle is given by

$$(3) \qquad D = 1 - \frac{t_7}{T_s}$$

The SSI eight state with their corresponding output voltages in αβ coordinates, voltage across the inductor and inductor state are listed in Table 1.

Table 1. SSI voltage vectors with corresponding switching states, output voltages, and inductor voltage and state.

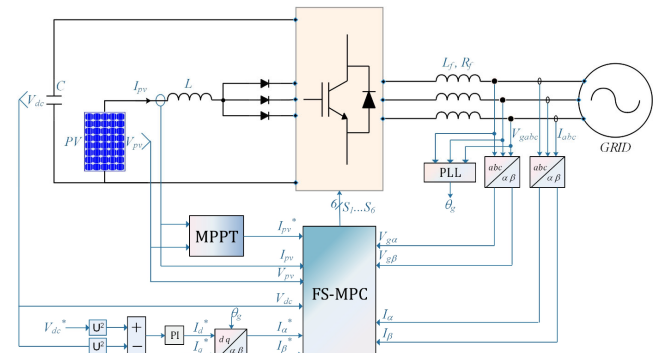| Voltage Vector	Switching state [S_1 S_2 S_3]	Inverter's output voltage [v_α v_β]	Inductor voltage	Inductor state
V_0	[0 0 0]	$[0\ \ 0]$	V_{in}	Charging
V_1	[1 0 0]	$[2/3V_{dc}\ \ 0]$	V_{in}	Charging
V_2	[1 1 0]	$[1/3V_{dc}\ \ \sqrt{3}/3V_{dc}]$	V_{in}	Charging
V_3	[0 1 0]	$[-1/3V_{dc}\ \ \sqrt{3}/3V_{dc}]$	V_{in}	Charging
V_4	[0 1 1]	$[-2/3V_{dc}\ \ 0]$	V_{in}	Charging
V_5	[0 0 1]	$[-1/3V_{dc}\ \ -\sqrt{3}/3V_{dc}]$	V_{in}	Charging
V_6	[1 0 1]	$[1/3V_{dc}\ \ -\sqrt{3}/3V_{dc}]$	V_{in}	Charging
V_7	[1 1 1]	$[0\ \ 0]$	$V_{in} - V_{dc}$	Discharging

Fig.2. Block diagram of the proposed FCS-MPC for PV grid connected SSI.

When the power converter is connected to the grid, as shown in the block diagram of Fig.2, the dynamics of the output currents in stationary reference frame αβ can be written as

$$(4) \qquad \dot{i}_{\alpha\beta} = Ai_{\alpha\beta} + B(v_{\alpha\beta} - V_{g\alpha\beta})$$

Where $A = \begin{bmatrix} -\dfrac{R_f}{L_f} & 0 \\ 0 & -\dfrac{R_f}{L_f} \end{bmatrix}$ and $B = \begin{bmatrix} \dfrac{1}{L_f} & 0 \\ 0 & \dfrac{1}{L_f} \end{bmatrix}$

$v_{\alpha\beta}$ and $V_{g\alpha\beta}$ are inverter output voltages, and grid voltages in αβ coordinates, respectively.

Maximum power point tracker (MPPT)

The highly non-linear characteristics curves of PV arrays are affected by irradiance and temperature variations. Therefore, MPPT is required in order to overcome these issues, and ensure that the PV operates all the time at the MPP. [1–3]

An MPPT algorithm should satisfactorily address the tradeoff between the fast dynamics and steady state oscillations [3].

Among several MPPT techniques, Perturb and Observe (P&O) is one of the most widely used algorithms due to its simplicity and low cost. [1–3]
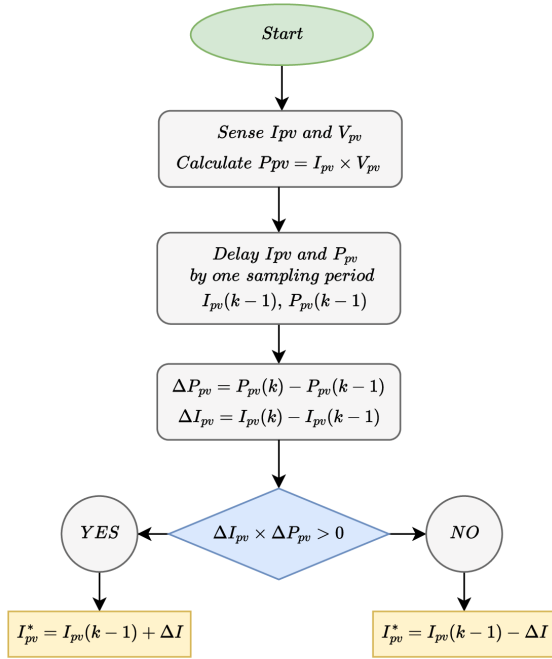
Fig.3. Flowchart of P&O MPPT algorithm.

However, conventional P&O algorithm suffers from poor tracking of MPP and high power oscillations in the steady state. These drawbacks, are mainly because of the fixed perturbation step size of conventional P&O.
Using a suitable PV model [12], Fig.4 Shows PV power and its slope to PV current. It is obvious from the graphs that when the operating point is far from the MPP, the perturbation is higher in order to converge rapidly. However, when being near to the MPP, the perturbation is too small to reduce power oscillations.

In this work, a low cost, improved P&O MPPT algorithm named as Variable Step-Size P&O (VSS-P&O) is considered. This algorithm uses the same principle of P&O but with a variable step size that is calculated automatically at each sampling time according to the operating point by using the derivative of power to current as [3,13,14]:

$$(5) \quad \Delta I = N \times \left| \frac{dP_{pv}}{dI_{pv}} \right| = N \times \left| \frac{P_{pv}(k) - P_{pv}(k-1)}{V_{pv}(k) - V_{pv}(k-1)} \right|$$

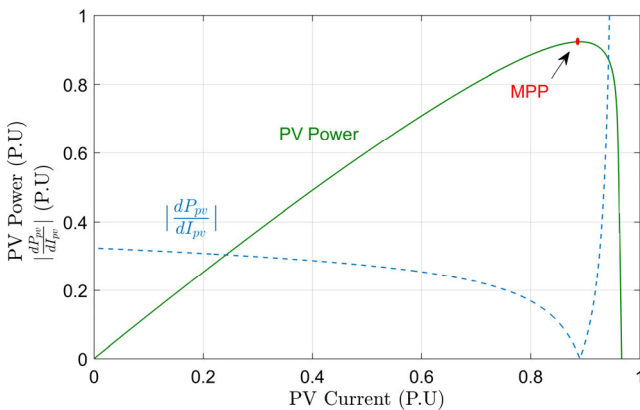Where N is a tuning parameter to adjust to step size.

Fig.4. Normalized PV power, and absolute slope of power versus current.

DC-Bus voltage control
The DC bus capacitor acts as a buffer between the input source and the output. Using the power conservation

principle, the power balance can be given by

$$(6) \quad P_{dc} = -P_g + P_{pv}$$

Where P_{pv}, P_g, P_{dc} are the PV power, Grid power, and the DC bus power, respectively.

Equation (5) can be written as

$$(7) \quad \frac{C}{2} \frac{dV_{dc}^2}{dt} = -\frac{3}{2} V_{gd} I_d + V_{pv} I_{pv}$$

Where I_d, V_{gd} are the grid current and voltage in dq frame.

By taking the PV power in the last equation as a disturbance, the DC bus voltage can be controlled by acting upon the grid current in the dq coordinates I_d using a simple Proportional-Integral (PI) controller as

$$(8) \quad I_d^* = k_p (V_{dc}^{*2} - V_{dc}^2) + k_i \int (V_{dc}^{*2} - V_{dc}^2)$$

Where k_p, k_i are the PI controller proportional and integral gains, respectively.

Reactive power control
The reactive power in the stationary reference frame dq can be expressed as:

$$(9) \quad Q = \frac{3}{2} \left[I_d . V_{gq} - I_q V_{gd} \right]$$

Moreover, knowing that $V_{gq} = 0$, Since the grid voltage vector is aligned on the d-axis of the dq reference frame, the reactive power in equation (9) will be

$$(10) \quad Q = -\frac{3}{2} I_q V_{gd}$$

Consequently, unity power factor operation of the proposed system can be achieved by setting the reactive power reference to zero, more precisely setting the q-axis current reference to zero. However, recent grid codes in some countries require that grid-tied distributed generators should participate in the grid energy management by absorbing or injecting an amount of reactive power.
From equation (10), the reactive power can be controlled by acting upon the q-axis grid current component I_q taking into account that the grid voltage V_{gd} is constant.

Finite control set-model predictive control
The proposed FCS-MPC is shown in Fig.5; the basic principle of the MPC controller is the prediction of the future behavior of the controlled variables, then, an optimization criterion of the control method is expressed as a cost function to be minimized [15].
Prediction model
Using the first-order Euler approximation, the discrete time model of (4) can be derived. This model is used to predict the future values of the output currents as

$$(11) \quad i_{\alpha\beta}(k+1) = (I + AT_s).i_{\alpha\beta}(k) + BT_s(v_{\alpha\beta} - V_{g\alpha\beta})$$

On the other hand, the dynamic equation of the inductor voltage for switching states V_0 to V_6 is

$$(12) \quad \frac{di_{pv}}{dt} = \frac{V_{pv}}{L}$$

And for switching state V_7 is

$$(13) \quad \frac{di_{pv}}{dt} = \frac{V_{pv} - V_{dc}}{L}$$

Therefore, Using Euler's approximation, the predicted values of the input inductor current are given by

$$(14)\, i_L(k+1) = \begin{cases} \dfrac{T_s}{L}V_{pv} + i_{pv}(k) & for \quad V_0...V_6 \\[2mm] \dfrac{T_s}{L}(V_{pv} - V_{dc}) + i_{pv}(k) & for \quad V_7 \end{cases}$$

Cost function

There are several ways to define a cost function which depends on the nature of the different terms involved in the formulation [15]. A suitable cost function for the studied system can be defined as the sum of quadrature weighted errors of the controlled variables

$$(15) \qquad g_i = (i^*_{\alpha\beta} - i_{\alpha\beta})^2 + \lambda(I^*_{pv} - I_{pv})^2$$

Where λ is a weighting factor that is used to favor a variable over the other.

However, since the two controlled variables have equal importance, the weighting factor is only used to compensate their difference of range [16]. Since the two controlled variables have equal importance, the weighting factor is only used to compensate their difference of range [9]. Finally, the action that minimizes the cost function is selected and applied in the next sampling period. The detailed steps of FCS-MPC controller are recapitalized in the following algorithm.

Algorithm 1. Proposed MPC algorithm

1: Function Predictive control() Sampling at T_s

Input: $I_{pv}(k), V_{pv}(k), V_{dc}(k), I_{\alpha\beta}(k), V_{g\alpha\beta}(k), I_{\alpha\beta ref}(k)$

2: Conversion from *abc* to *αβ* frame

$$x_{\alpha\beta,} = Kx_{abc,} \left| x \in \left\{ I_{\alpha\beta}, V_{g\alpha\beta}, I_{\alpha\beta ref} \right\} \right.$$

3: *Loop-1:* Predictive control & Cost function computation
for: i = 1,…,8:
 grid current prediction model:
  $i_{\alpha\beta}(k+1)_i \Longleftarrow$ Compute from (9)
 PV current prediction model:
  $i_L(k+1)_i \Longleftarrow$ Compute from (12)
end for
4: *Loop-2:* Cost function minimization

$g_{min} \leftarrow \infty$

for: i = 1,…,8:
 if $g(i) < g_{min}$, **then**
  $g_{min} \leftarrow g(i)$
 end if
end for
5: Return switching state
Return **S_i** (switching state corresponding to *i*, generating minimum error)
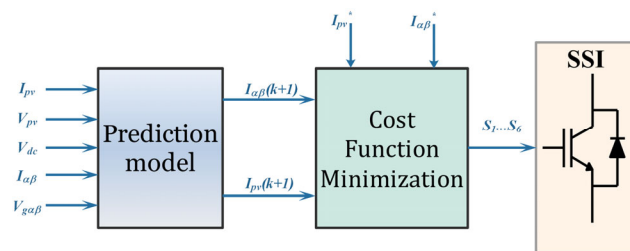
end function

Fig.5. Proposed predictive controller scheme.

Simulation results

In order to validate the proposed control technique for the studied system, a numerical simulation using 'Simpower systems' of MATLAB/Simulink® has been accomplished. The used PV panel consists of (3 series) × (6 parallel) PV modules of 120W each (type: siemens BPSX-120). The rest of system parameters are listed in Table 2.

Table 2. Simulation parameters

Parameter	Value
Grid voltage V_{abc}	120 V_{RMS} (L-L)
Frequency f	50 Hz
PV maximum power @STC P_{MPP}	2160 W
PV Current at MPP @STC I_{MPP}	21.3 A
PV Voltage at MPP @STC V_{MPP}	101.1 V
DC-Bus capacitor C	1100 µF
Input inductor L	10 mH
Output inductor L_f	5 mH
Controller sampling time T_s	20 µs

To assess the robustness of the proposed controllers, the irradiance profile is chosen to be constant from 0 s to 0.45 s and from 0.5 s to 0.7 s with 1000W/m² and 750 W/m², respectively, varying progressively between 1000w/m² and 750 W/m² from 0.45 s to 0.5 s, and suddenly changing from 750 W/m² to 1000 W/m² at 0.7s as shown in the irradiance profile of Fig.6. For this first test, unity power factor operation is considered, so the reactive power reference is set to 0.
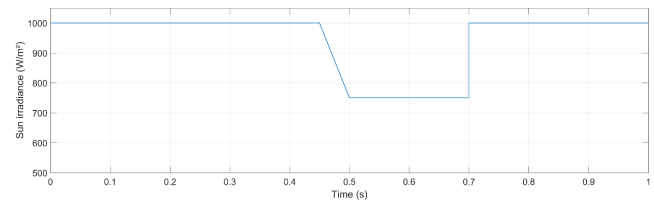

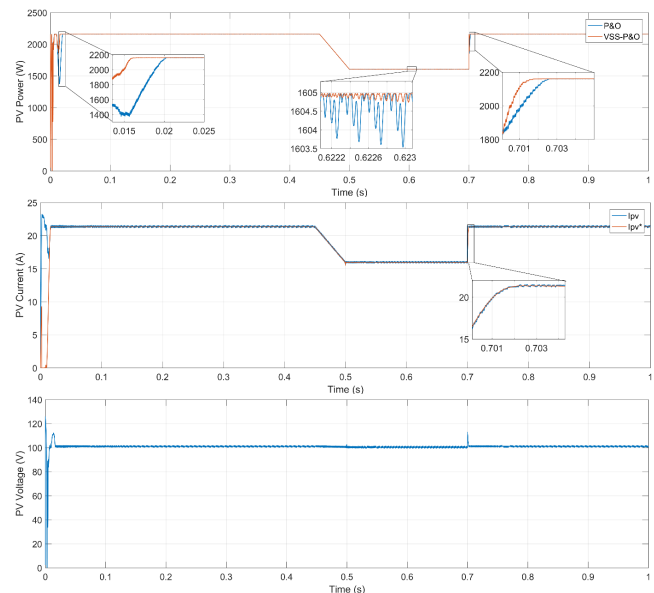Fig.6. Sun irradiance profile.

Fig.7. Waveforms of (a) PV Power, (b) PV current with its reference, (c) PV voltage.

Fig.7. (a) shows that the power delivered by the PV with conventional P&O and VSS-P&O MPPT algorithms. It can be observed that the PV power reaches its MPP faster for

VSS-P&O and with lower steady state oscillations when compared with conventional P&O. Taking into consideration that PV power is controlled thanks to predictive current controller which has succeeded in keeping the PV current tracking its reference generated by the MPPT algorithm Fig 7. (b).
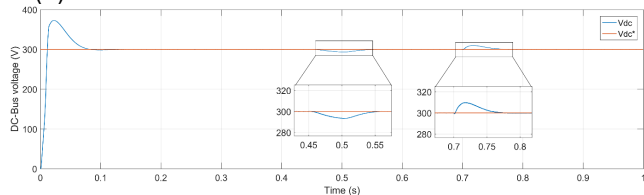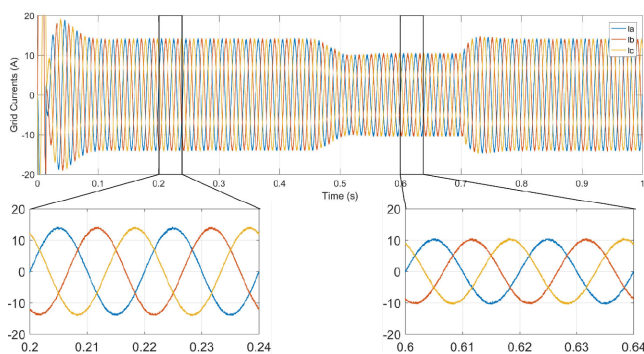

Fig.8. DC-Bus voltage with its reference.

Fig.9. Grid currents waveforms.

The DC bus voltage shown by Fig.8 is tracking the reference set to 300 V rapidly and accurately even during changing in solar irradiance. Furthermore, as compared with PV voltage of Fig.7. (c) which is about 100 V, it can be confirmed the boosting ability of the SSI.

The three-phase grid current shown in Fig.9 are practically sinusoidal, low distorted, and in agreement with standards. The total harmonic distortion (THD) is lower than 5% (varies depending on the operating point between 1.65% and 2.5%) as depicted by the THD and harmonics spectra of Fig.10. Additionally, it is obvious from active and reactive powers in Fig.11. that unity power factor operation is achieved, where reactive power is almost around zero as result of the decoupled power controller. However, non-unity power factor operation could be considered by changing the reactive current reference as shown in the second test.
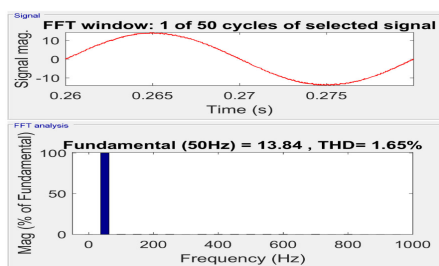

Fig.10. Phase (a) grid current THD, and harmonics spectra.
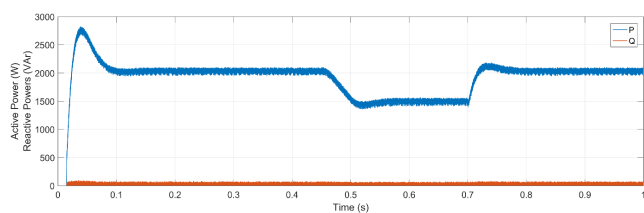

Fig.11. Active and reactive powers waveforms.

To evaluate the decoupled power control of the proposed controller, a second test has been conducted. In this instance, the system is configured to exchange reactive power with the electrical grid. For this test, a new irradiance profile is considered. From 0 s to 0.4 s, the irradiance is 0 W/m² to simulate nighttime conditions. After 0.4 s, the irradiance varies as shown in Fig.12.
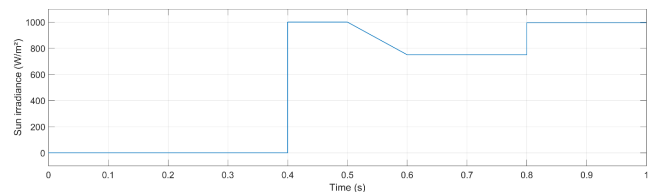

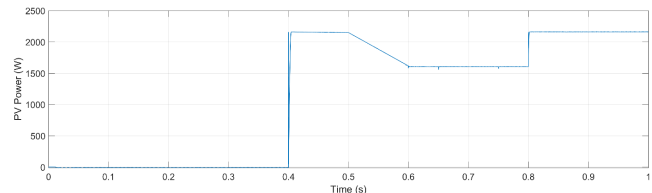Fig.12. Second test irradiance profile.

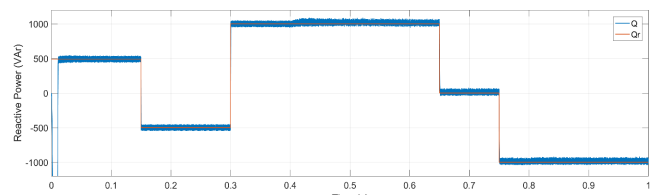Fig.13. PV power waveform.

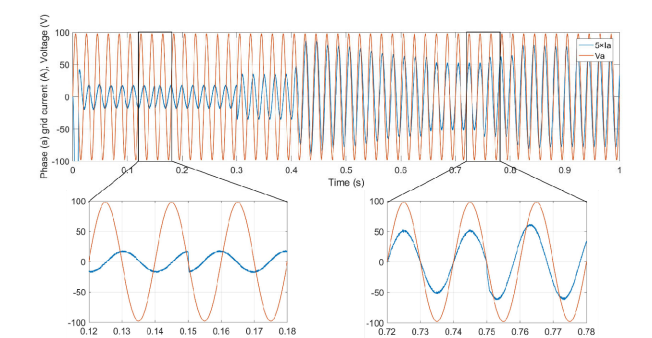Fig.14. Reactive power waveform with its reference.

Fig.15. Phase (a) grid current and voltage waveforms.

Fig.13. shows the PV power, Fig.14. shows the reactive power, whereas Fig.15. exhibits the grid currents. In this simulation all the possible scenarios have been evaluated. From 0 s to 0.4 s there is no irradiance so the PV panel is not generating any power. However, the reactive power is varying rapidly and following its reference perfectly with low oscillations from 500 VAr to -500 VAr and to 1000 VAr at 0.1s, 0.15s, and 0.3s, respectively. During this time since there is no active power the SSI is working as reactive power compensator. From 0.4s to 1s the reactive power is maintained at 1000 VAr until 0.65s and then varying to zero and -500 VAr, during this time the irradiance is changing between 1000 W/m² and 750 W/m². It is obvious from PV power waveform that it is tracking its MPP and it is neither affected by the control of reactive power nor affecting it, which confirms the decoupled power control.

Grid currents in this second test are always sinusoidal and low distorted all along simulation time. In Fig.15. it is shown that grid currents respond quickly to sudden reactive power reference changes by changing their phase shifts as exhibited by the zoom under the figure.

In the zoom of left, the current is lagging the voltage by π/2 since the system is injecting reactive power (positive reactive power reference) until 0.15s where it will be leading

the voltage by π/2 because now the system is absorbing reactive power (negative reactive power reference).

In the zoom of right, the current starts in phase with the voltage because the reactive power is set to zero (unity power factor operation) until 0.75 s where a phase shift appears due to reactive power reference changing to a negative value which means absorbing reactive power.

Conclusion

This paper presented a grid connected PV system controlled by MPC using an SSI. Since the SSI has boosting capabilities, the PV conversion chain is on single stage configuration which is better compared with other two stages configurations especially in terms of lower complexity and higher power efficiency. In order to ensure that the PV operates all the time at its maximum power point, a simple but effective current based variables step-size P&O MPPT algorithm is used to generate the reference current for the MPC controller. Furthermore, a linear PI controller is employed for the control of DC Bus voltage. The whole system is controlled by an FCS-MPC that has as objectives to control the input PV current and the output grid currents. The simulation results demonstrate the feasibility of the system and the good performance of the proposed techniques.

Authors

Dr. Hamza FEROURA, Department of Electronics, Laboratory of Power Electronics and Industrial Control (LEPCI), University of Setif-1, Setif, Algeria, E-mail: hamzaferoura@hotmail.com;
Pr. Fateh KRIM, Department of Electronics, Laboratory of Power Electronics and Industrial Control (LEPCI), University of Setif-1, Setif, Algeria, E-mail: krim_f@ieee.org;
Dr. Abdelouahad MAY, Department of Electronics, Laboratory of Power Electronics and Industrial Control (LEPCI), University of Setif-1, Setif, Algeria, E-mail: essbadro94@gmail.com;
Dr. Abdesslam BELAOUT, Research Center in Industrial Technologies CRTI, Algiers, Algeria, E-mail: belaout_s@yahoo.fr.

REFERENCES

[1] Kumar, L. A., Alexander, S. A., & Rajendran, M. (2020). Power electronic converters for solar photovoltaic systems. Academic Press.
[2] Abu-Rub, H., Malinowski, M., & Al-Haddad, K. (2014). Power electronics for renewable energy systems, transportation and industrial applications. John Wiley & Sons.
[3] Femia, N., Petrone, G., Spagnuolo, G., & Vitelli, M. (2017). Power electronics and control techniques for maximum energy harvesting in photovoltaic systems. CRC press.
[4] Abdelhakim, A., Mattavelli, P., & Spiazzi, G. (2015). Three-phase split-source inverter (SSI): Analysis and modulation. IEEE Transactions on Power Electronics, 31(11), 7451-7461.
[5] Abdelhakim, A., Mattavelli, P., Boscaino, V., & Lullo, G. (2017). Decoupled control scheme of grid-connected split-source inverters. IEEE Transactions on Industrial Electronics, 64(8), 6202-6211.
[6] Elthokaby, Y., Abdelsalam, I., Abdel-Rahim, N., & Mohamed, I. (2023). Standalone PV-based single-phase split-source inverter using model-predictive control. Alexandria Engineering Journal, 62, 357-367.
[7] Cocco, G. M., Grigoletto, F. B., Scherer, L. G., & de Camargo, R. F. (2022). Modeling and control of hydro-pv hybrid power system with three-phase three-leg split-source inverter. Journal of Control, Automation and Electrical Systems, 33(5), 1563-1575.
[8] Nannam, H. C., Banerjee, A., & Guerrero, J. M. (2021). Analysis of an interleaved control scheme employed in split source inverter based grid-tied photovoltaic systems. IET Renewable Power Generation, 15(6), 1301-1314.
[9] Hassan, M. S., Abdelhakim, A., Shoyama, M., Imaoka, J., & Dousoky, G. M. (2020). Three-phase split-source inverter-fed PV systems: Analysis and mitigation of common-mode voltage. IEEE Transactions on Power Electronics, 35(9), 9824-9838.
[10] Guler, N., & Komurcugil, H. (2021). Energy function based finite control set predictive control strategy for single-phase split source inverters. IEEE Transactions on Industrial Electronics, 69(6), 5669-5679.
[11] Güler, N. (2022). Multi-objective cost function based finite control set-sliding mode control strategy for single-phase split source inverters. Control engineering practice, 122, 105114.
[12] Villalva, M. G., Gazoli, J. R., & Ruppert Filho, E. (2009). Comprehensive approach to modeling and simulation of photovoltaic arrays. IEEE Transactions on power electronics, 24(5), 1198-1208.
[13] Ahmed, J., & Salam, Z. (2018). An enhanced adaptive P&O MPPT for fast and efficient tracking under varying environmental conditions. IEEE Transactions on Sustainable Energy, 9(3), 1487-1496.
[14] Soni, A. K., Jana, K. C., & Gupta, D. K. (2023). Variable step-size adaptive maximum power point tracking algorithm for solar cell under partial shading conditions. IETE Journal of Research, 69(3), 1562-1577.
[15] Rodriguez, J., & Cortes, P. (2012). Predictive control of power converters and electrical drives. John Wiley & Sons.
[16] Cortés, P., Kouro, S., La Rocca, B., Vargas, R., Rodríguez, J., León, J. I., ... & Franquelo, L. G. (2009, February). Guidelines for weighting factors design in model predictive control of power converters and drives. In 2009 IEEE International Conference on Industrial Technology (pp. 1-7). IEEE.